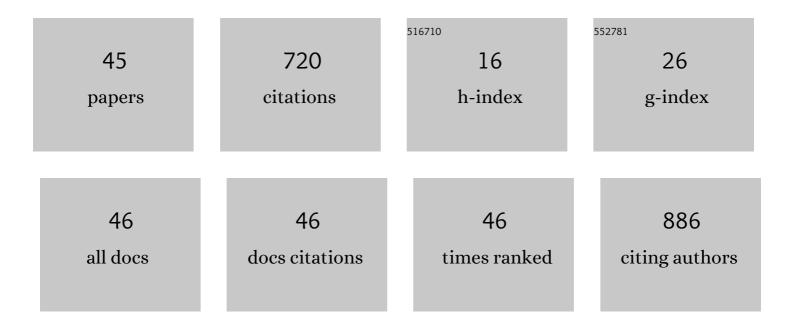
Ajeet Srivastav

List of Publications by Year in descending order

Source: https://exaly.com/author-pdf/1910111/publications.pdf Version: 2024-02-01



AIFET SDIVASTAV

| # | Article | IF | CITATIONS |
|----|--|-----|-----------|
| 1 | Thermodynamic model to predict bulk metallic glass forming composition in Zr-Cu-Fe-Al system and understanding the role of Dy addition. Physica B: Condensed Matter, 2022, 624, 413416. | 2.7 | 10 |
| 2 | Formation mechanism of nanocrystalline W derived cubic-H0.5WO3. Scripta Materialia, 2022, 208, 114363. | 5.2 | 4 |
| 3 | Understanding the Growth Mechanism of Hematite Nanoparticles: The Role of Maghemite as an Intermediate Phase. Crystal Growth and Design, 2021, 21, 16-22. | 3.0 | 9 |
| 4 | Review: Oxygen-deficient tungsten oxides. Journal of Materials Science, 2021, 56, 6615-6644. | 3.7 | 40 |
| 5 | Unveiling the crystallographic origin of mechanochemically induced monoclinic to triclinic phase transformation in WO ₃ . CrystEngComm, 2021, 23, 1821-1827. | 2.6 | 6 |
| 6 | Kinetics and phase formation during crystallization of Hf64Cu18Ni18 amorphous alloy. Phase Transitions, 2021, 94, 110-121. | 1.3 | 2 |
| 7 | Kinetic Approach to Determine the Class-Forming Ability in Hf-Based Metallic Glasses. Metallurgical and Materials Transactions A: Physical Metallurgy and Materials Science, 2021, 52, 1169-1173. | 2.2 | 4 |
| 8 | Corrosion Studies of Hf64Cu18Ni18 Metallic Glass in Acidic and Alkaline Media. Transactions of the Indian Institute of Metals, 2021, 74, 949-956. | 1.5 | 2 |
| 9 | On the temperature dependent magnetization in dual-phase Co nanowires confinedly electrodeposited inside nanoporous alumina membrane. Journal of Crystal Growth, 2021, 562, 126084. | 1.5 | 5 |
| 10 | Unraveling the growth mechanism of W18O49 nanowires on W surfaces. CrystEngComm, 2021, 23, 6559-6566. | 2.6 | 3 |
| 11 | Understanding the strain-dependent structure of Cu nanocrystals in Ag–Cu nanoalloys. Physical Chemistry Chemical Physics, 2021, 23, 26165-26177. | 2.8 | 5 |
| 12 | Crystallite size induced bandgap tuning in WO3 derived from nanocrystalline tungsten. Scripta Materialia, 2020, 176, 47-52. | 5.2 | 20 |
| 13 | Microstructure evolution and densification during spark plasma sintering of nanocrystalline W-5wt.%Ta alloy. Philosophical Magazine Letters, 2020, 100, 442-451. | 1.2 | 3 |
| 14 | Graphene-based chemiresistive gas sensors. Comprehensive Analytical Chemistry, 2020, , 149-173. | 1.3 | 6 |
| 15 | WO3.1/3H2O nanorods/nanoplates: Growth mechanism and CO2 uptake. Materialia, 2020, 14, 100943. | 2.7 | 2 |
| 16 | Measurements of the melting points, liquidus, and solidus of the Mo, Ta, and Mo Ta binary alloys using a novel high-speed pyrometric technique. International Journal of Refractory Metals and Hard Materials, 2020, 93, 105335. | 3.8 | 9 |
| 17 | Graphene/chitosan-functionalized iron oxide nanoparticles for biomedical applications. Journal of Materials Research, 2019, 34, 3389-3399. | 2.6 | 17 |
| 18 | Effect of Re on microstructural evolution and densification kinetics during spark plasma sintering of nanocrystalline W. Advanced Powder Technology, 2019, 30, 2779-2786. | 4.1 | 14 |

AJEET SRIVASTAV

| # | Article | IF | CITATIONS |
|----|---|------|-----------|
| 19 | Localized pore evolution assisted densification during spark plasma sintering of nanocrystalline W-5wt.%Mo alloy. Scripta Materialia, 2019, 159, 41-45. | 5.2 | 20 |
| 20 | Estimation of diffusivity from densification data obtained during spark plasma sintering. Scripta Materialia, 2019, 161, 36-39. | 5.2 | 17 |
| 21 | Graphene from discharged dry cell battery electrodes. Journal of Hazardous Materials, 2019, 366, 358-369. | 12.4 | 45 |
| 22 | Antioxidant efficacy of chitosan/graphene functionalized superparamagnetic iron oxide nanoparticles. Journal of Materials Science: Materials in Medicine, 2018, 29, 154. | 3.6 | 14 |
| 23 | Applicability of γ* Parameter on Glass Forming Ability of Zr-,Ti-,Hf-(Cu–Ni)-based Metallic Glasses. Transactions of the Indian Institute of Metals, 2018, 71, 2839-2843. | 1.5 | 0 |
| 24 | In-situ \$\$hbox {TiO}_{2}\$\$ TiO 2 –rGO nanocomposites for CO gas sensing. Bulletin of Materials Science, 2018, 41, 1. | 1.7 | 23 |
| 25 | Thermodynamic calculation and experimental validation of Hf-rich glass forming compositions in Hf-Cu-Ni system. Journal of Non-Crystalline Solids, 2018, 500, 191-195. | 3.1 | 25 |
| 26 | Novel coalescence-driven grain-growth mechanism during annealing/spark plasma sintering of NiO nanocrystals. Journal of the European Ceramic Society, 2017, 37, 4973-4977. | 5.7 | 7 |
| 27 | Modeling and Theory: general discussion. Faraday Discussions, 2016, 186, 371-398. | 3.2 | 1 |
| 28 | Synthesis of Nanoparticle Assemblies: general discussion. Faraday Discussions, 2016, 186, 123-152. | 3.2 | 0 |
| 29 | Applications to Soft Matter: general discussion. Faraday Discussions, 2016, 186, 503-527. | 3.2 | 1 |
| 30 | Nanocomposites: general discussion. Faraday Discussions, 2016, 186, 277-293. | 3.2 | 1 |
| 31 | Evolution of morphology and texture during high energy ball milling of Ni and Ni-5 wt%Cu powders. Materials Characterization, 2016, 120, 90-96. | 4.4 | 10 |
| 32 | Formation of amorphous alumina during sintering of nanocrystalline B2 aluminides. Materials Characterization, 2016, 119, 186-194. | 4.4 | 7 |
| 33 | Crystallographic-shear-phase-driven W18O49 nanowires growth on nanocrystalline W surfaces. Scripta Materialia, 2016, 115, 28-32. | 5.2 | 19 |
| 34 | Nucleation and growth mechanism of Co–Pt alloy nanowires electrodeposited within alumina template. Journal of Nanoparticle Research, 2015, 17, 1. | 1.9 | 4 |
| 35 | On correlation between densification kinetics during spark plasma sintering and compressive creep of B2 aluminides. Scripta Materialia, 2015, 107, 63-66. | 5.2 | 15 |
| 36 | Grain-size-dependent non-monotonic lattice parameter variation in nanocrystalline W: The role of non-equilibrium grain boundary structure. Scripta Materialia, 2015, 98, 20-23. | 5.2 | 36 |

AJEET SRIVASTAV

| # | Article | IF | CITATIONS |
|----|--|-----|-----------|
| 37 | On Joule heating during spark plasma sintering of metal powders. Scripta Materialia, 2014, 93, 52-55. | 5.2 | 61 |
| 38 | Crystal anisotropy induced temperature dependent magnetization in cobalt nanowires electrodeposited within alumina template. Journal of Magnetism and Magnetic Materials, 2014, 349, 21-26. | 2.3 | 20 |
| 39 | XRD Characterization of Microstructural Evolution During Mechanical Alloying of W-20Âwt%Mo. Transactions of the Indian Institute of Metals, 2013, 66, 409-414. | 1.5 | 16 |
| 40 | Dilatometric analysis on shrinkage behavior during non-isothermal sintering of nanocrystalline tungsten mechanically alloyed with molybdenum. Journal of Alloys and Compounds, 2012, 536, S41-S44. | 5.5 | 15 |
| 41 | Initial-stage Sintering Kinetics of Nanocrystalline Tungsten. Metallurgical and Materials Transactions A: Physical Metallurgy and Materials Science, 2011, 42, 3863-3866. | 2.2 | 24 |
| 42 | Magnetic nanowires by electrodeposition within templates. Physica Status Solidi (B): Basic Research, 2010, 247, 2364-2379. | 1.5 | 139 |
| 43 | Molten salt electrolysis of neodymium: electrolyte selection and deposition mechanism. Institutions of Mining and Metallurgy Transactions Section C: Mineral Processing and Extractive Metallurgy, 2010, 119, 88-92. | 0.6 | 16 |
| 44 | Loading Rate Sensitivity of Jute/Glass Hybrid Reinforced Epoxy Composites: Effect of Surface Modifications. Journal of Reinforced Plastics and Composites, 2007, 26, 851-860. | 3.1 | 21 |
| 45 | Tribological and Morphological Evaluation of Ni-P and Ni-P/D Coatings. Materials Science Forum, 0, 969, 73-79. | 0.3 | 2 |